IOPscience iopscience.iop.org

Home Search Collections Journals About Contact us My IOPscience

R-matrix with Pseudo-States (RMPS) method: application to CH^+ resonances curves

This article has been downloaded from IOPscience. Please scroll down to see the full text article.

2011 J. Phys.: Conf. Ser. 300 012017

(http://iopscience.iop.org/1742-6596/300/1/012017)

View the table of contents for this issue, or go to the journal homepage for more

Download details:
IP Address: 2.102.169.212
The article was downloaded on 31/07/2011 at 20:07

Please note that terms and conditions apply.

Journal of Physics: Conference Series **300** (2011) 012017 doi:10.1088/1742-6596/300/1/012017

R-matrix with Pseudo-States (RMPS) method: application to CH^+ resonances curves

Dermot Madden, Jonathan Tennyson and Rui Zhang

Department of Physics and Astronomy, University College London, Gower St., London WC1E 6BT, UK

E-mail: d.madden@ucl.ac.uk, j.tennyson@ucl.ac.uk

Abstract.

In a series of calculations on both electron and positron collisions with small molecules the R-Matrix with Pseudo-States (RMPS) method has been found to recover polarisation effects neglected in other close-coupling methods including the standard R-matrix procedure. The molecular R-Matrix and RMPS methods is being applied to determine low-lying resonance states of CH^+ as a function of internuclear separation. Initial results are presented for both a standard R-matrix close-coupling model and for an RMPS calculation. Eigenphase sums and resonances below the $^3\Pi$ threshold are presented for $^2\Pi$ total symmetry. These resonances are classified by their quantum defects and compared to previous results. Prospects for these and other calculations using the RMPS method are discussed.

1. Introduction

The R-matrix method provides a rigorous *ab initio* procedure for studying electron molecule collisions and, in the context of dissociative recombination (DR), for providing resonance curves and widths ("couplings"). For few-electron targets the method has been shown to give highly accurate results [1, 2, 3]. However for many-electron targets the standard implementation of the R-matrix method can struggle to fully converge polarisation effects; a feature shared with other close-coupling methods, see the comparison given by refs. [4, 5, 6] for example.

R-matrix calculations have been used as the basis for successful studies of DR [7, 8, 9]. However for many-electron targets it has proved necessary to "calibrate" [8] the resonance curves, for example using spectroscopic data. Since the method is essentially variational, these curves are systematically too high in energy. This problem can only be cured using a more complete treatment of polarisation effects.

The R-matrix with pseudo-states (RMPS) method was introduced by Gorfinkiel and Tennyson [6, 10] initially to extend the range of electron-collision calculations above the target ionisation threshold and to treat the ionisation process itself. It was however rapidly realised that the method also gave a significantly improved treatment of target

Published under licence by IOP Publishing Ltd

polarisation. Recently this has been explicitly demonstrated in a systematic study of the polarisability of small molecules [11].

The RMPS method has been used to model and characterise resonance effects in electron impact detachment of C_2^- [12, 13]. It has been shown to give excellent results for low energy collisions with the highly polarisable Li_2 molecule [14]. Perhaps most impressively, the method has been used to compute positron – molecule cross sections which reproduce the measurements, see Figure 1. These studies also yield greatly enhanced positron annihilation rates in line with observations. Both these processes are particularly poorly modelled by conventional R-matrix calculatins [15, 16].

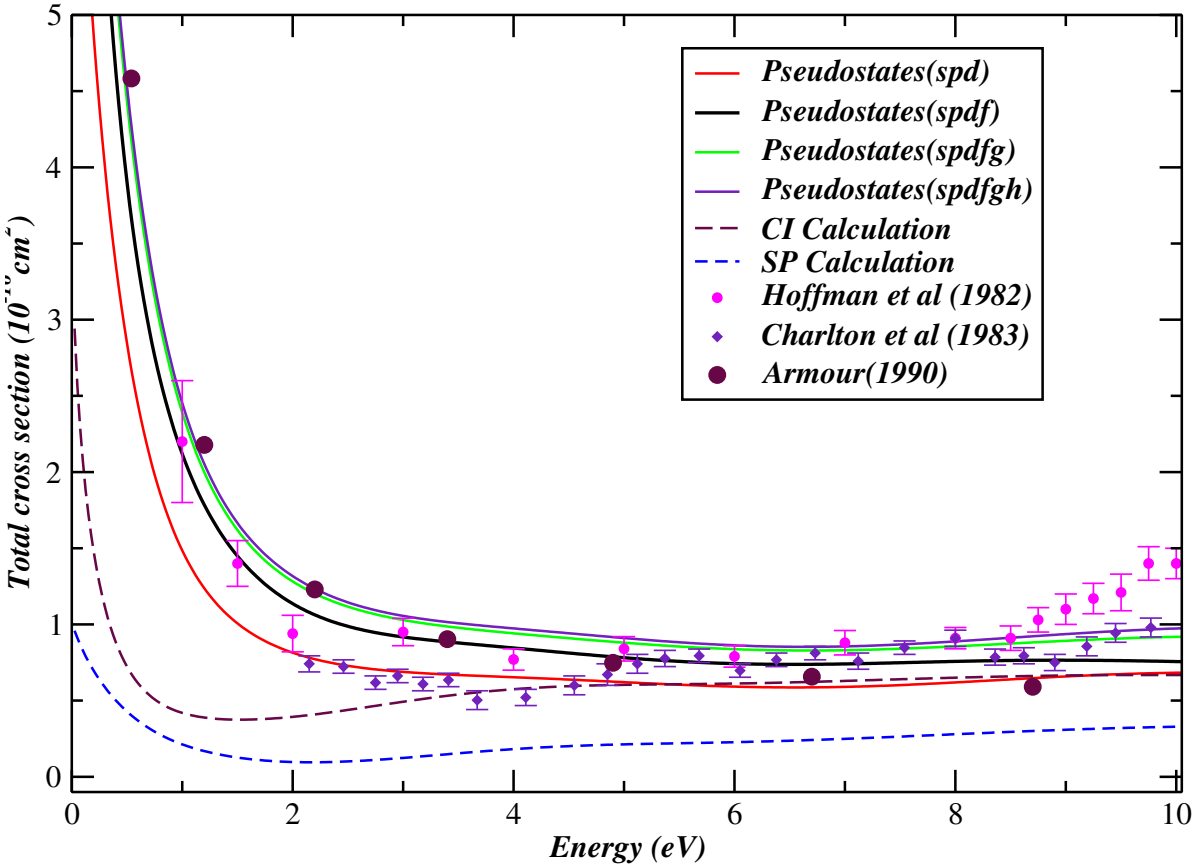

Figure 1. Positron – H_2 elastic cross sections. Solid curves are RMPS calculations with angular functions with $\ell \leq 2$ to $\ell \leq 5$ due to Zhang *et al* [17]; long dash curve is a standard R-matrix close coupling calculation; short dash curve is for a static plus polarisation R-matrix calculation. Hoffmann *et al* [18] and Charlton *et al* [19] are measured cross sections. Armour *et al* [20] are calculations which used wavefunctions that explicitly include the positron-electron coordinate but only consider Σ_g^+ symmetry scattering. The rise in the observed cross section at higher energies is caused by the onset positronium formation at energies above 7 eV.

Given the sucess of the RMPS method, it is natural to ask whether its use can improve predictions of DR resonance curves. To study this we have chosen to look at electron collisions with CH^+.

CH^+ is one of many molecules important for astrophysical observations and is of interest for the formation of large hydrocarbons in the interstellar medium. A key feature of work on CH^+ has being its observed overabundance in the interstellar medium compared to calculated predictions [21]. Our aim is to use *ab initio* methods to look at dissociative recombination of CH^+. There have been a number of previous theoretical [22, 23] and experimental [24, 25, 26] studies of this problem. However there remains issues with the accurate prediction of the rate of dissociative recombination under astrophysical conditions. This could potentially have a large impact on the overall abundance of CH^+ in the interstellar medium. In this report we present preliminary results from our study.

2. Method

The R-Matrix approach is based on dividing configuration space into two regions. The inner region is defined by a sphere of radius a, centred at the centre-of-mass of the molecule. This sphere is chosen to enclose the target charge distribution. In the inner region the interactions are strong and multi-centred and include both exchange and correlation between the scattered electron and the electrons of the target. In the outer region, exchange and correlation effects are neglected as only the long range multi-pole potential is important. For electron-CH^+ scattering, the long-range Coulomb forces are accounted for by the use of Coulomb functions in the asymptotic region; the main issue is therefore to account for the effects of the target dipole moment at long-range.

The R-matrix method, in common with other close-coupling methods, only includes a finite number of states in the close-coupling expansion. It therefore, of necessity, does not account for higher-lying target states or the targer continuum. Intermediate energy processes, where the collision energy lies near to or above the ionisation threshold, cannot be treated correctly without accounting for these states. The RMPS method includes an extra pseudo-continuum basis set which allows for the construction of an extra set of target states. These are refered to as pseudostates as they are not true eigenstates of the target molecule, but they can, if selected correctly, be used to describe the missing electronic target states and the continuum which is discretized within the R-matrix sphere.

The previous R-matrix study of resonance curves in the CH^+ system used Slater Type Orbitals (STOs) to represent the target and numerical functions for the continuum [27]. Since the RMPS method is only implemented in the polyatomic R-matrix code [28], both target, continuum and, indeed, pseudo-continuum orbitals are represented using Gaussian Type Orbitals (GTOs). For continuum orbitals GTOs up to and including g waves were used [29]. The polyatomic R-matrix code cannot treat linear symmetries and all calculations were performed in C_{2v} symmetry. It is reasonably straightforward to reconstruct the full symmetry from these calculations particularly since considerable care was taken to ensure that the calculation preserved the degeneracy structure of the calculations.

One of us has recently written a comprehensive review of molecular R-matrix calculations [30] and the reader is refered there for further details of the method.

3. Target calculations

The CH^+ target was represented in the R-Matrix and RMPS calculations using a cc-pVTZ basis set, a radius of 12 a_0 for the R-matrix box and keeping the two lowest electrons frozen for the calculations. For the standard R-matrix calculation we used a complete active space (CAS) configuration interaction (CI) space of $(1a_1)^2$(2-$4a_1$,$1b_1$,$1b_2$)^4. For the RMPS calculation we added a pseudo-continuum orbital basis of 10s,10p,6d orbitals, with exponents generated using α=0.17 and β=1.4. The RMPS configuration is $(1a_1)^2$(2-$4a_1$,$1b_1$,$1b_2$)^3 (5-$14a_1$,2-$7b_1$,2-$7b_2$,1-$3a_2$)^1.

Potential energy curves for CH^+ for the four lowest states: the X $^1\Sigma$ ground state, a $^3\Pi$, A $^1\Pi$ and b $^3\Sigma^+$ were compared with the high accuracy electronic structure calculations of Barinvos and Van Hemert [31]. The upper and lower panels of Figure 2 show these curves for the R-Matrix and RMPS methods respectively. The RMPS run shows a clear improvement in these energy curves. In the R-Matrix data the $^3\Pi$ and $^1\Pi$ curves dissociate to a slightly lower energy than the $^3\Sigma$ and $^1\Sigma$ curves. In the RMPS run this divergence disappears and the four curves dissociate correctly to the same limit ($C^+(^2P)$ + $H(^2S)$).

The calculations of Barinvos and Van Hemert used a cc-pV6Z basis set with with added diffuse functions and polarisation functions to account for the core polarisation. The comparison of the RMPS calculation with these results confirms that the overall shape of our curves are broadly correct with a smaller basis set (cc-pVTZ) and calculation. The remaining discrepency in the curves appears to be caused by the fact that our RMPS curves slightly underestimate the dissociation energy of CH^+.

4. Scattering calculations

Many models were tested but only results for close-coupling calculations using the standard R-matrix and RMPS target models specified above will be given. The RMPS calculations retained 47 states, $6(^1\Sigma^+)$, $7(^3\Sigma^+)$, $8(^1\Pi)$, $9(^3\Pi)$, $5(^1\Sigma^-)$, $7(^3\Sigma^-)$, $3(^1\Delta)$, $2(^3\Delta)$, cutting off at 43.3 eV above the ground state. The outer region R-matrices were propagated to a radius of $100a_0$.

Figure 3 shows eigenphase sums with $^2B_1$ ($^2\Pi$) symmetry for the standard and RMPS calculations. Both methods shows the very complicated resonance structures which converge on the first excitation threshold, a $^3\Pi$. However the lower (and more realistic) threshold for this state in the RMPS study leads to a significant compressed energy scale.

A challenge is presented by the need to resolve the dense collection of resonances just below the $^3\Pi$ threshold. The present calculations use the module in the UK R-Matrix polyatomic code called RESON [32] which automatically fits the eigenphase sums to a

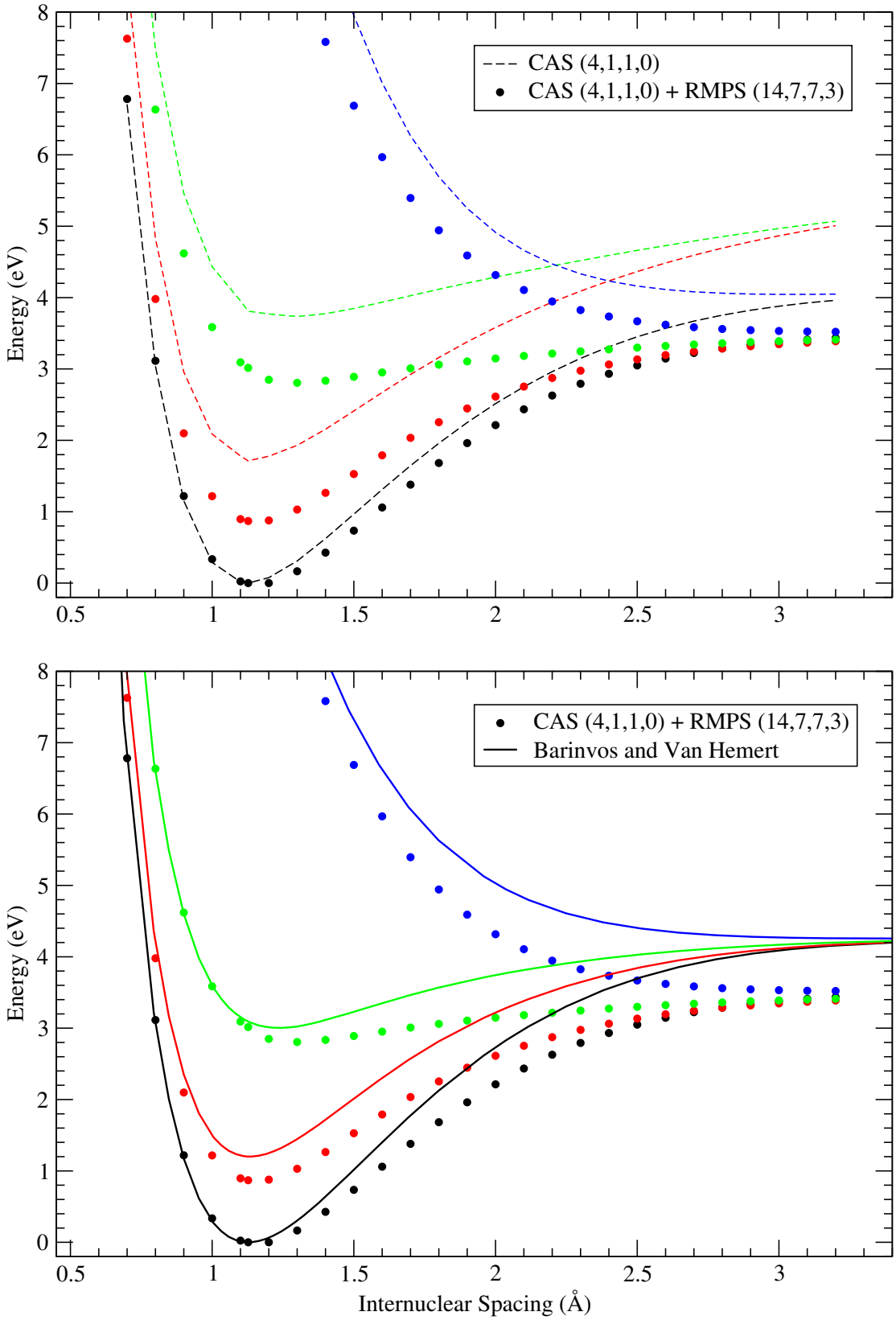

Figure 2. Potential energy curves for the four lowest electronic states of CH^+. Both figures show the following states assending in the order $^1\Sigma^+$, $^3\Pi$, $^1\Pi$ and $^3\Sigma^+$. Upper figure, CAS-CI calculation and RMPS Calculation. Lower figure: RMPS calculation and calculations by Barinvos and Van Hemert [31]. In all cases zero energy has been set to minimum of the ground state.

Breit-Wigner form in a recursive fashion. These resonance parameters are then used to generate complex quantum defects. Future work will examine use of a similar automated implementation of the time-delay method [33, 34] which has been shown to better resolve densely packed resonances. However, use of the time-delay method has a price in terms of speed and efficiency as it requires some hand intervention to produce results. A direct search for the resonances as poles in the complex-energy S-matrix will also be investigated. This method is particularly appropriate for an R-matrix implementation since it is only necessary to consider complex energies in the outer region [35]. Similarly the QB method [36] provides an R-matrix specific resonance characterisation procedure.

Analysis of the resonances allow us to identify four distinct series which we can tentatively assign as being the sσ, pσ, dσ and dδ series. Resonances associated with f and g waves have essentially zero quantum defect which means that their resonances coincide making them difficult to resolve with a Briet-Wigner fit. Figure 4 shows how our calculated quantum defects vary with bondlength in R-Matrix calculations, the results shown in this figure are from a R-Matrix calculation that used the DZP basis set, a larger CAS of $(1a_1)^2$(4-8a_1,1-3b_1,1-3b_2,1-1a_2)^4 and retained 15 states in the scattering calculation.

An alternative method of matching resonances below the $^3\Pi$ threshold between neighbouring geometries is to plot their quantum defects using Edlén plots. These plots show the quantum defects of each resonance against the resonance energies relative to the threshold energy. Figure 5 shows such plots for the sσ series for the standard R-Matrix and RMPS calculations. This figure clearly shows the increase of the quantum defects obtained with the RMPS calculations.

Table 1 compares our quantum defects for the (a $^3\Pi$)*n*pσ those of Carata *et al* [37] at the CH^+ equilibrium bondlength. Table 2 gives our effective quantum numbers of the bound states which form the ($X^1\Sigma^+$)*n*pσ series.

Table 1. Quantum defects for the (a $^3\Pi$)*n*pσ series at R=1.127Å from our R-Matrix, RMPS calculations and the multichannel quantum defect of the series from Carata *et al* [37].

n	RMPS	R-Matrix	Carata et al.
5	0.8361		
6	0.8212	0.5069	
7	0.8126	0.5341	
8	0.8078	0.5430	
9	0.8052	0.5477	
10		0.5509	
11	0.8052	0.5534	
MQDT			0.8530

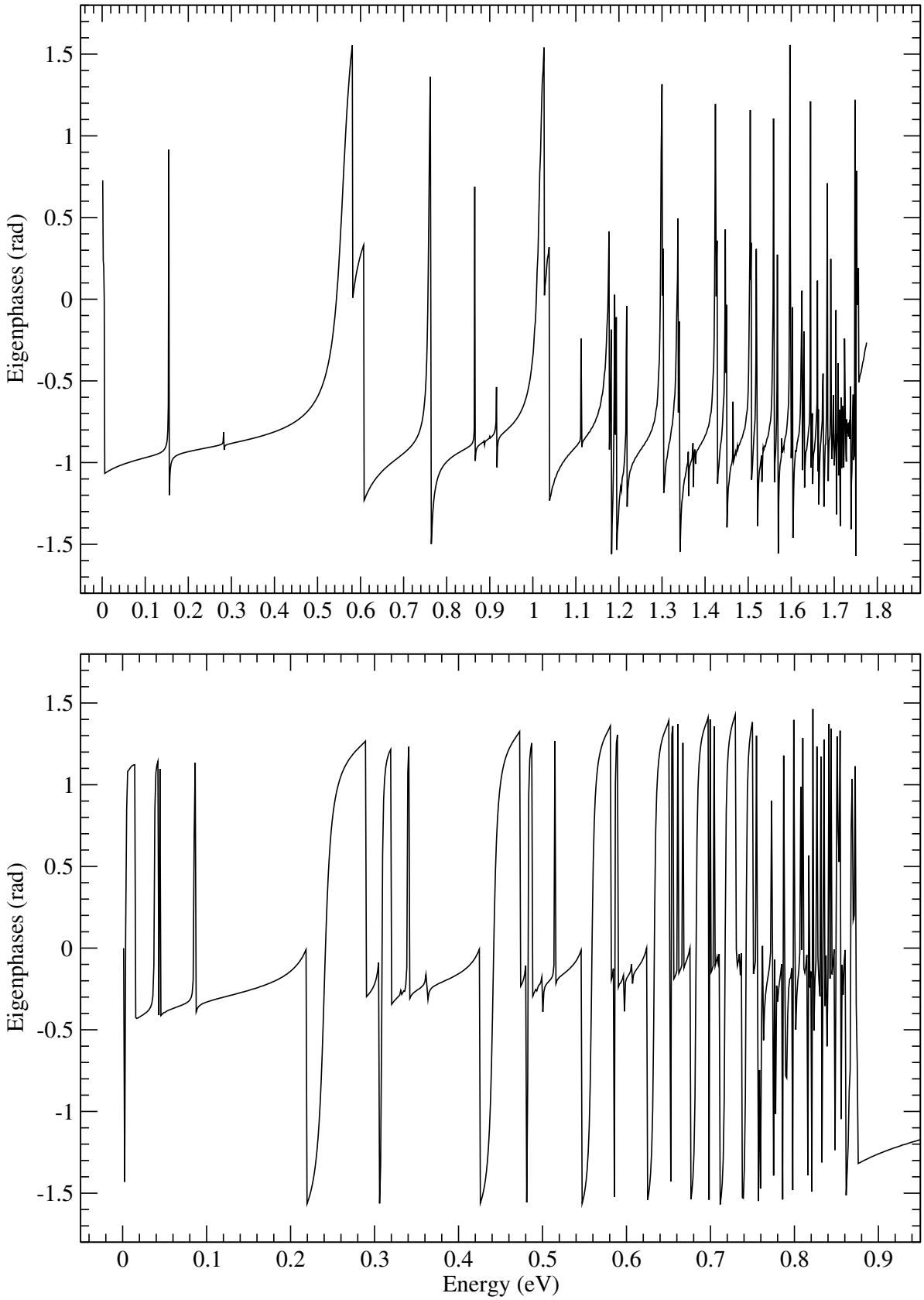

Figure 3. Eigenphases at equilibrium (R = 1.127Å) from the standard R-Matrix calculation (upper figure) and the RMPS calculation (lower figure). Note that in the R-Matrix calculation the $^3\Pi$ threshold is at 1.76 eV and in the RMPS calculation 0.87 eV.

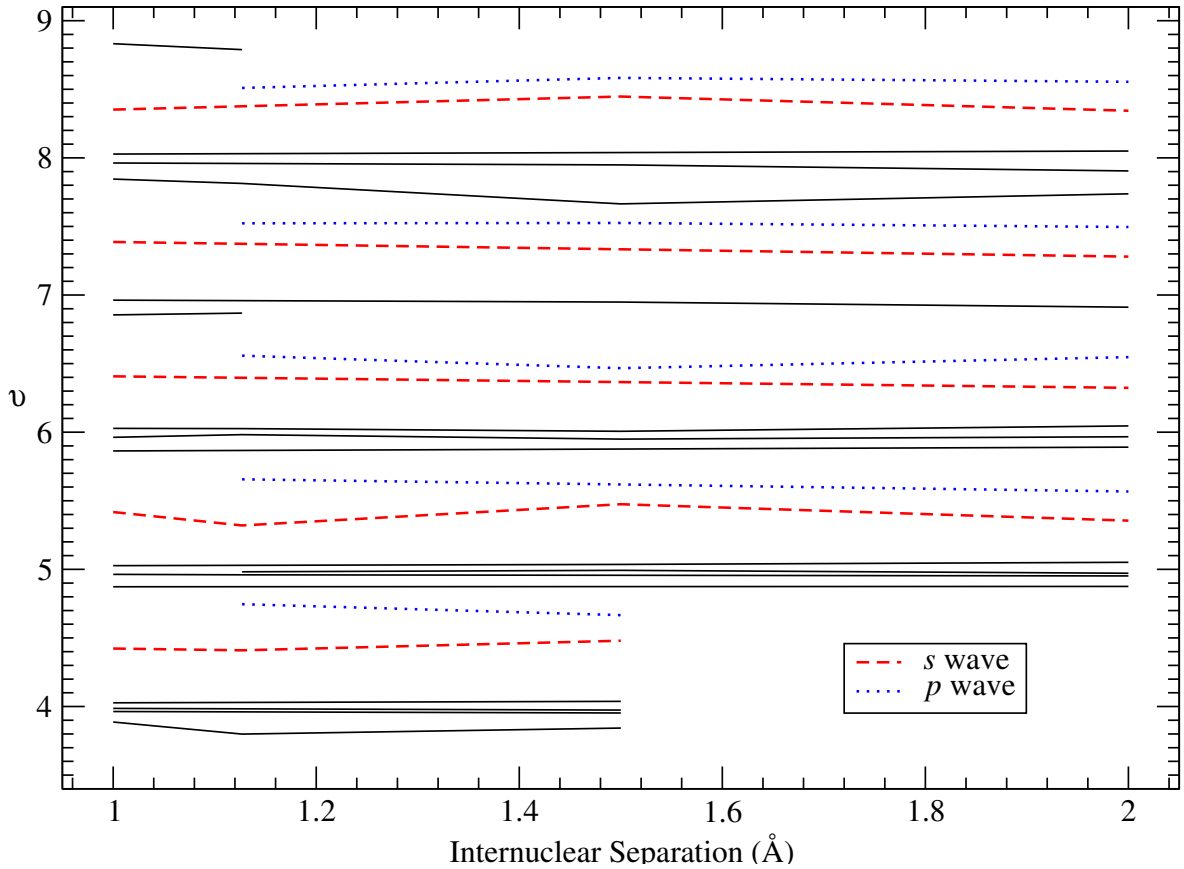

Figure 4. Effectuve quantum number, ν as a function of geometry for the R-Matrix calculations

Table 2. Effective Quantum Numbers for the $(^1\Sigma^+)np\sigma$ series at R=1.127Å, from R-Matrix and RMPS Calculations

RMPS	R-Matrix
4.685	
5.682	
6.672	
7.658	7.727
	8.682
9.612	9.660
10.571	10.647
11.505	11.639

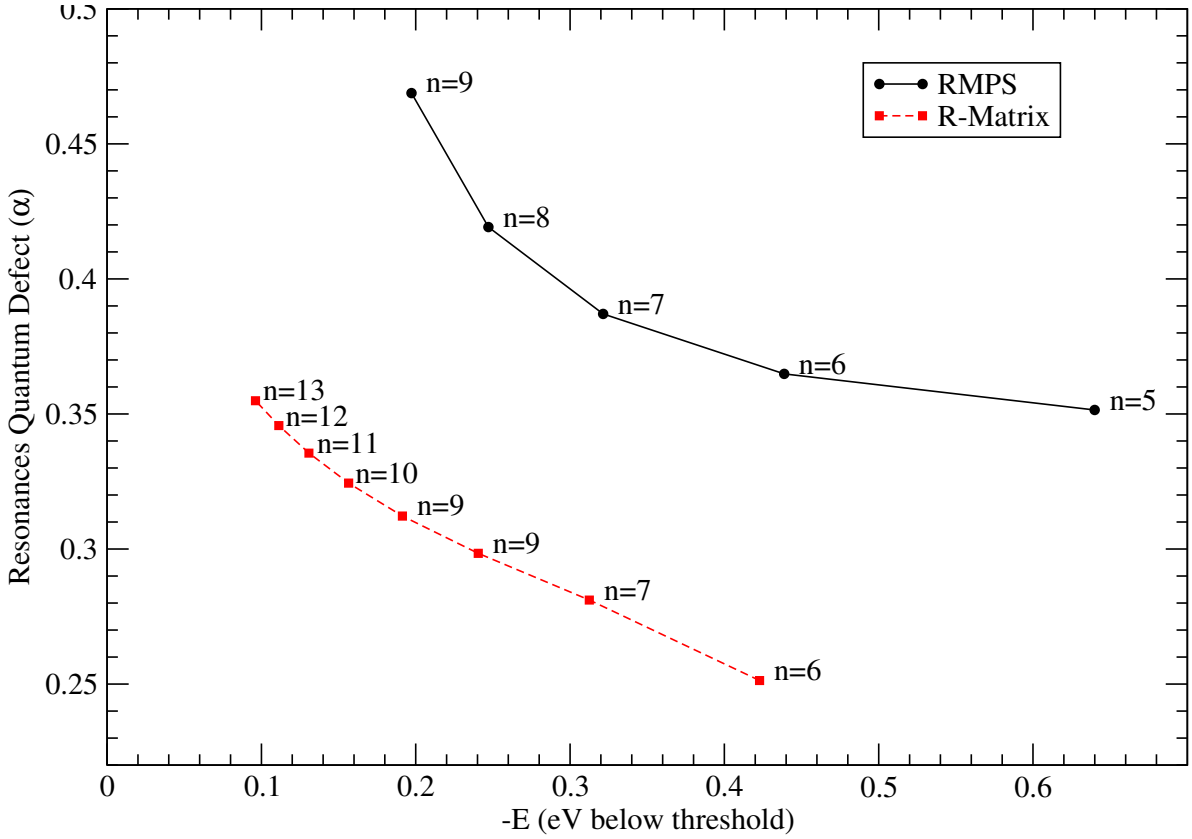

Figure 5. R-Matrix and RMPS Edlén plot at R=1.127Å, for the $(a^3\Pi)ns\sigma$ series. The Edlén plot shows the quantum defects in order of decending effective quantum number, by plotting the quantum defect, α, against the resonance position below the threshold.

5. Future Work

We have confirmed that the RMPS method is capable of giving significantly improved results for resonances in the CH system using a reduced model. Our next goal is to construct a final, large model which can be used to produce reliable data on these features. These resonances will then be analysised using a variety of methods, including the Timedel[34] module, with the aim of fully to resolving all the structures in the region of dense resonances just below the threshold. This should allow more accurate resolving of the crossing points of key resonances and the energy curves.

Acknowledgements

DM thanks EPSRC for PhD funding, and the US National Science Foundation and NASA for travel support.

References

[1] Tennyson J and Noble C J 1985 *J. Phys. B: At. Mol. Phys.* **18** 155–165

[2] Sarpal B K, Branchett S E, Tennyson J and Morgan L A 1991 *J. Phys. B: At. Mol. Opt. Phys.* **24** 3685–3699
[3] Tennyson J 1996 *At. Data Nucl. Data Tables* **64** 253–277
[4] Orel A E 1992 *Phys. Rev. A* **46** 1333
[5] Faure A and Tennyson J 2002 *J. Phys. B: At. Mol. Opt. Phys.* **35** 1865–1873
[6] Gorfinkiel J D and Tennyson J 2004 *J. Phys. B: At. Mol. Opt. Phys.* **37** L343–L350
[7] Sarpal B K, Tennyson J and Morgan L A 1994 *J. Phys. B: At. Mol. Opt. Phys.* **27** 5943–5953
[8] Schneider I F, Rabadán I, Carata L, Tennyson J, Andersen L H and Suzor-Weiner A 2000 *J. Phys. B: At. Mol. Opt. Phys.* **33** 4849–4861
[9] Motapon O, Fifirig M, Florescu A, Waffeu-Tamo F O, Crumeyrolle O, Varin-Breant G, Bultel A, Vervisch P, Tennyson J and Schneider I F 2006 *Plasma Phys. Science Technology* **15** 23–32
[10] Gorfinkiel J D and Tennyson J 2005 *J. Phys. B: At. Mol. Opt. Phys.* **38** 1607–1622
[11] Jones M and Tennyson J 2010 *J. Phys. B: At. Mol. Opt. Phys.* **43** 045101
[12] Halmová G and Tennyson J 2008 *Phys. Rev. Lett.* **100** 213202
[13] Halmová G, Gorfinkiel J D and Tennyson J 2008 *J. Phys. B: At. Mol. Opt. Phys.* **41** 155201
[14] Tarana M and Tennyson J 2008 *J. Phys. B: At. Mol. Opt. Phys.* **41** 205204
[15] Danby G and Tennyson J 1990 *J. Phys. B: At. Mol. Opt. Phys.* **23** 1005–1016 erratum 23, 2471 (1990)
[16] Franz J, Baluja K L, Zhang R and Tennyson J 2008 *Nucl. Instr. Meths. Phys. Res. B* **266** 419–424
[17] Zhang R, Baluja K L, Franz J and Tennyson J *J. Phys. B: At. Mol. Opt. Phys.*
[18] Hoffman K R, Dababneh M S, Hsieh Y, Kauppila W E, Pol V, Smart J H and Stein T S 1982 *Phys. Rev. A* **25** 1393–1403
[19] Charlton M, Griffith T C, Heyland G R and Wright G L 1983 *J. Phys. B: At. Mol. Phys* **16** 323–341.
[20] Armour E A G, Baker D J and Plummer M 1990 *J. Phys. B: At. Mol. Phys* **23** 3057–3074
[21] Pineau des Forets G, Flower D R, Hartquist T W and Dalgarno A 1986 *Mon. Not. R. astr. Soc* **220** 801–824
[22] Giusti-Suzor A and Lefebvre-Brion H 1977 *Astrophys. J.* **214** 101–103
[23] Takagi H, Kosugi N and Le Dourneuf M 1991 *J. Phys. B: At. Mol. Phys.* **24** 711–732
[24] Amitay Z, Zajfman D, Forck P, Hechtfischer U, Seidel B, Grieser M, Habs D, Repnow R, Schwalm D and Wolf A 1996 *Phys. Rev. A* **54** 4032
[25] Mul P M, Mitchell J B A, D'Angelo V S, Defrance P and McGowan J W 1981 *J. Phys. B: At. Mol. Phys.* **14** 1353–1361
[26] Forck P, Broude C, Grieser M, Habs D, Kenntner J, Liebmann J, Repnow R, Amitay Z and Zajfman D 1994 *Phys. Rev. Lett.* **72** 2002–2005
[27] Tennyson J 1988 *J. Phys. B: At. Mol. Opt. Phys.* **21** 805–816
[28] Morgan L A, Tennyson J and Gillan C J 1998 *Computer Phys. Comms.* **114** 120–128
[29] Faure A, Gorfinkiel J D, Morgan L A and Tennyson J 2002 *Computer Phys. Comms.* **144** 224–241
[30] Tennyson J 2010 *Phys. Rep.* **491** 29–76
[31] Barinovs G and van Hemert M C 2004 *Chem. Phys. Lett.* **399** 406–411
[32] Tennyson J and Noble C J 1984 *Computer Phys. Comms.* **33** 421–424
[33] Stibbe D T and Tennyson J 1996 *J. Phys. B: At. Mol. Opt. Phys.* **29** 4267–4283
[34] Stibbe D T and Tennyson J 1998 *Computer Phys. Comms.* **114** 236–242
[35] Noble C J, Dörr M and Burke P G 1993 *J. Phys. B: At. Mol. Opt. Phys.* **26** 2983–3000
[36] Quigley L and Berrington K 1996 *J. Phys. B: At. Mol. Opt. Phys.* **29** 4529–4542
[37] Carata L, Orel A E, Raoult M, Schneider I F and Suzor-Weiner A 2000 *Phys. Rev. A* **62** 052711